ISSN: 1410-8917
e-ISSN: 2597-9914

Jurnal Kimia Sains dan Aplikasi 27 (8) (2024): 363-370

Jurnal Kimia Sains dan Aplikasi
Journal of Scientific and Applied Chemistry

Journal homepage: http://ejournal.undip.ac.id/index.php/ksa

Photodegradation of Methylene Blue Dye Using $BiVO_4$/g-C_3N_4 Composites under Visible Light Irradiation

Anung Riapanitra [1], Tien Setyaningtyas [1], Ghinatanitha Haqqu Haryadinaru [1,*]

[1] Department of Chemistry, Faculty of Mathematics and Natural Sciences, Jenderal Soedirman University, Purwokerto, Indonesia

* Corresponding author: ghinatanitha02@gmail.com

https://doi.org/10.14710/jksa.27.8.363-370

Article Info

Article history:

Received: 14th June 2024
Revised: 03rd August 2024
Accepted: 08th August 2024
Online: 31st August 2024

Keywords:
Methylene blue; $BiVO_4$/g-C_3N_4; photocatalysis; heterojunction; g-C_3N_4

Abstract

This study evaluates the degradation of methylene blue through photocatalysis using $BiVO_4$/g-C_3N_4 material with the help of visible light. Material characterization was conducted using X-ray diffraction, scanning electron microscopy, and UV-Vis diffuse reflectance spectroscopy data. The characterization results show that the crystal structure of $BiVO_4$/g-C_3N_4 is a heterojunction between monoclinic $BiVO_4$ and hexagonal g-C_3N_4, with a crystal size of about 10.16 nm and a band gap energy value of about 2.16 eV. The morphology formed is a combination of sheet and rod-like. This study optimized the photocatalytic activity of the composite by analyzing the variation of g-C_3N_4 concentration, degradation time, and methylene blue pH. The results show that the $BiVO_4$/g-C_3N_4 sample has optimal photocatalytic and adsorption properties in sample B (1:3) with pH 7 and a degradation time of 150 minutes. Under these conditions, the $BiVO_4$/g-C_3N_4 composite successfully degraded methylene blue by 94.14%. The rate kinetics of the photocatalytic reaction followed first order, with *OH species playing the most role in the degradation mechanism. These findings highlight the potential of $BiVO_4$/g-C_3N_4 as an effective photocatalyst material for organic pollutant degradation applications, offering a sustainable solution for wastewater treatment.

1. Introduction

Synthetic dyes in modern industry have reached more than 700,000 tons annually, with the textile sector being the most significant consumer [1]. Synthetic dyes such as methylene blue (MB) are essential in various industries, but MB is known for its toxic, carcinogenic, and non-biodegradable properties [2]. This causes severe threats to human health and the environment, such as respiratory distress, blindness, and decreased aquatic biodiversity. Waste treatment methods such as advanced oxidation and electrochemical degradation are often expensive and complex [3].

MB dye removal methods from water include advanced oxidation, ultra-filtration, electrochemical degradation, coagulation-flocculation, and adsorption processes. However, these methods often have disadvantages, such as high operational costs and require advanced procedures, making them less effective [4]. Photodegradation is a relatively cheap and easy-to-implement method, effectively removing color and converting dye molecules into simple, non-toxic, inorganic compounds such as CO_2 and H_2O. Photocatalysts typically are semiconductor materials activated by photons and are used to accelerate reactions without reacting. Examples of photocatalysts include TiO_2, ZnO, CdS, ZnS, and $BiVO_4$ [5]. Based on the research of Ganeshbabu *et al.* [6], $BiVO_4$ is a superior photocatalyst with a band gap of 2.4 eV that can absorb visible light and has high photocatalysis efficiency and strong oxidation-reduction potential, effective in degrading complex organic compounds. However, according to the continuous research of Jin *et al.* [7], $BiVO_4$ has a shortcoming in that its electron transfer efficiency is low, leading to electron-hole recombination and lowering the photocatalyst efficiency. To overcome this problem, structural modification or adding other materials is required to improve its electron transfer efficiency.

g-C_3N_4, or graphite carbonitride, is an attractive semiconductor with a band gap of about 2.7-2.8 eV, allowing visible light absorption and giving it high photocatalytic potential. Its 2D structure offers a large surface area and high electron mobility, allowing electrons to move efficiently. In addition, g-C_3N_4 has high chemical and thermal stability, making it resistant to various conditions [8]. Compositing $BiVO_4$ with g-C_3N_4 can improve the photocatalysis performance of $BiVO_4$ by forming a heterojunction. In this composite, g-C_3N_4 is a sensitizer to increase light absorption or a cocatalyst to enhance electron transfer [9].

This study aims to synthesize the photocatalyst $BiVO_4$ composited with g-C_3N_4, focusing on particle size, morphology control, and photocatalyst applications under visible light. It is expected that the synergistic effect of g-C_3N_4 composite will increase the photodegradation activity of MB, offering an effective solution for the treatment of synthetic dye waste in the textile industry.

2. Experimental

2.1. Materials

The materials used in this study were melamine (Loba Chemie, Germany), ammonium metavanadate (NH_4VO_3) (analytical reagent, Aldrich, USA), bismuth (III) nitrate pentahydrate ($Bi(NO_3)_3.5H_2O$) (analytical reagent, Merck, Germany), sodium hydroxide (NaOH) (analytical reagent, Merck, Germany). Demineralized water, distilled water, methylene blue dye (Merck, Germany), hydrochloric acid (HCl) pickling agent (Merck, Germany), absolute ethanol (Merck, Germany), methanol (Merck, Germany), benzoquinone (Aldrich, USA), isopropanol (Merck, Germany), ammonium oxalate (Merck, Germany), and filter paper (Whatman, UK).

2.2. Synthesis of $BiVO_4$/g-C_3N_4 Composite

$BiVO_4$ was synthesized according to previous research with modifications [10]. In this process, 4.3863 g $Bi(NO_3)_3{\cdot}5H_2O$ and 0.3509 g NH_4VO_3 were dissolved in 100 mL of distilled water and stirred magnetically for 1 hour. The pH of the mixture was raised to 10 with 2.5 M NaOH and stirred for 30 minutes. Raising the pH in the synthesis of $BiVO_4$ is important to ensure the formation of a monoclinic phase that is more efficient in photodegradation. This alkaline condition accelerates the formation of the monoclinic phase with higher crystal stability than the tetragonal phase and increases the photocatalytic efficiency. The monoclinic structure has energy band and band-gap configurations that favor charge separation and absorption of visible light, thus improving the material's ability to decompose organic contaminants under light [11]. Then, the solution was put into an autoclave at 180°C for 14 hours; this process will accelerate the reaction and crystallization and produce a more stable $BiVO_4$ phase; the solution was then centrifuged, the precipitate was filtered, washed with ethanol and water for 3 times, dried at 60°C for 24 hours, and calcined at 400°C for 4 hours.

Meanwhile, g-C_3N_4 was synthesized through thermal condensation in which 5 g of melamine in a closed alumina crucible was heated at 550°C for 4 hours, then cooled to room temperature and pureed the g-C_3N_4 product. During heating, melamine undergoes decomposition and polycondensation reactions, connecting melamine units through triazine bonds and forming a planar network structure. This structure consists of repeated layers bonded together, where each triazine unit is connected to other triazine units in an arrangement similar to graphene, but with nitrogen replacing some of the carbon. This planar network has a stable and conductive structure, which gives g-C_3N_4 semiconductor properties with a band gap of about 2.7 eV, ideal for photocatalysis and adsorption applications [12].

$BiVO_4$/g-C_3N_4 composite was prepared by adding 0.2 g g-C_3N_4 into 20 mL of methanol, then stirring ultrasonically for 1 hour to exfoliate the g-C_3N_4. Next, 0.1 g $BiVO_4$ was added to the g-C_3N_4 suspension and stirred magnetically until the solvent evaporated. The formed composite was dried at 80°C and calcined at 300°C for 4 hours. This process was repeated with a $BiVO_4$/g- C_3N_4 mass ratio of 1:3 and 1:4.

2.3. Photocatalyst Material Characterization

The photocatalyst material was characterized using several techniques. A Scanning Electron Microscope (SEM) JEOL JSM-6520LA was employed to examine the surface morphology by scanning the sample with an electron beam, producing images that revealed the size and shape of the material grains. X-ray diffraction (XRD) analysis was conducted using a Shimadzu XRD-7000 to determine the crystal structure and purity of the material by measuring its diffraction pattern. The resulting data identified the material's crystal structure and phase. Additionally, UV-visible diffuse reflectance spectroscopy (UV-Vis DRS) using a JASCO V-670 was used to measure the reflection of UV and visible light, enabling the determination of the material's band gap energy, which is crucial for understanding how the material absorbs light.

2.4. Photocatalytic Study

The process of determining the optimum photocatalyst mass, pH, and reaction time for MB degradation began by adding 0.05 g of $BiVO_4$/g- C_3N_4 in ratios of 1:2, 1:3 and 1:4 to a glass cup containing 50 mL of 10 ppm MB solution. The solution was then stirred while irradiated under visible light for 150 minutes, and the absorbance was measured using a UV- visible spectrophotometer to evaluate the effectiveness of each photocatalyst ratio. Once the most effective photocatalyst ratio was determined, it was added to a beaker containing 50 mL of 10 ppm MB solution, and the pH of the solution was set at 3, 5, 7, 9, and 11. The solution was stirred under visible light for a preset duration, after which the absorbance was measured to determine the optimum pH for maximum MB degradation. In the final step, the photocatalyst was added to a beaker containing 50 mL of 10 ppm MB solution at the optimum pH. This mixture was stirred under visible light for varying intervals (30, 60, 90, 120, 150, 180, and 210 minutes), with absorbance measured every 30 minutes to identify the optimum time for the most efficient MB degradation.

The $BiVO_4/g-C_3N_4$ photocatalyst material at the optimum condition with the most significant dye %degradation was added to a glass cup containing 50 mL of 10 ppm MB solution at the optimum solution pH. Then, 0.2 mL of 0.25 M benzoquinone solution was added to test the catalytic function of superoxide radicals. The solution was stirred under dark conditions and room temperature for 30 minutes to achieve adsorption-desorption equilibrium, then irradiated for the optimum time under visible light. After that, samples of approximately 5 mL were taken, diluted by a factor of 2, and centrifuged to measure absorbance using a UV-visible spectrophotometer at the maximum wavelength. The process was repeated using 4 µL of isopropanol PA scavenger to test the catalytic function of hydroxyl radicals and 0.2 mL of 0.25 M ammonium oxalate scavenger to test the catalytic function of holes.

3. Results and Discussion

3.1. Crystal Phase Analysis of $BiVO_4/g-C_3N_4$ Material

The XRD analysis results obtained from the $g-C_3N_4$, $BiVO_4$, and $BiVO_4/g-C_3N_4$ composite samples in Figure 1 provide a deep insight into the crystal structure and its implications for photocatalytic properties.

Figure 1 reveals that the diffraction pattern of the $g-C_3N_4$ sample shows peaks at 2θ = 26.48° and 27.56°, corresponding to the (101) and (002) planes. This indicates that the diffraction peak aligns with the hexagonal phase of $g-C_3N_4$ (JCPDS No. 87-1526). The crystalline plane (101) with weak diffraction intensity consists of a fundamental structural unit (triazine ring) of a graphite phase carbon nitride layer, which follows a cyclic arrangement. This cyclic regulation refers to the electron transfer in the carbon and nitrogen atoms, which causes weak diffraction intensity. The crystal plane (002) with a strong peak is formed by the interplanar accumulation of the annular aromatic system, which has solid and stable properties [13].

The photocatalytic properties of $g-C_3N_4$ are strongly influenced by its crystal structure, especially the ordered layers on the (002) plane. This structure allows efficient light absorption, which is essential for generating electron-hole pairs. The absorbed light energy leads to the formation of electron-hole pairs that function in photocatalytic reactions. In addition, the ordered structure on the (002) plane increases the stability of the material, reducing charge recombination that often reduces the efficiency of photocatalysis. By ensuring that electrons and holes can stay longer and function optimally, $g-C_3N_4$ can utilize light energy effectively and improve performance in photocatalytic applications [14].

Table 1. Photocatalyst material crystal size

Sample	Crystal size (nm)
$g-C_3N_4$	4.00
$BiVO_4$	17.85
$BiVO_4/g-C_3N_4$	10.16

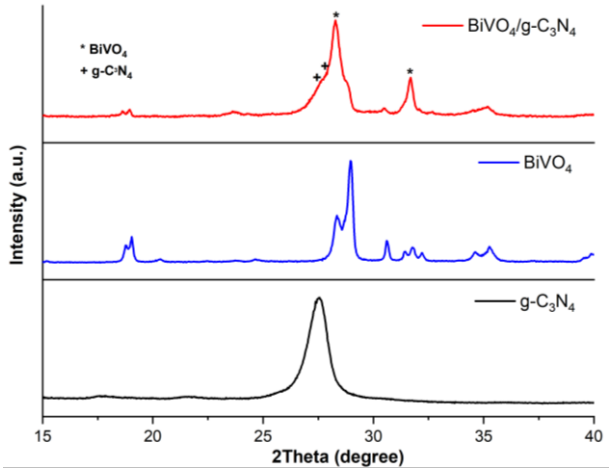

Figure 1. X-ray diffraction characterization

The monoclinic structure of the pure $BiVO_4$ sample in Figure 1 is obtained through its diffraction patterns observed at 2θ = 28.35°, 28.96°, 30.6° corresponds to the crystal planes (130), (121), and (040). All sharp diffraction patterns exhibit high crystalline properties with a monoclinic structure, and the results align with the standard values (JCPDS No. 14-0688). As for the $BiVO_4/g-C_3N_4$ composite sample, it was observed that all diffraction peaks produced the same index as $BiVO_4$ and $g-C_3N_4$. A slight shift in the diffraction peak indicates a strong interface interaction between $BiVO_4$ and $g-C_3N_4$.

The interface interaction between $BiVO_4$ and $g-C_3N_4$ in the photocatalytic system affects the efficiency and photocatalytic activity of the material. $BiVO_4$, has a monoclinic crystal structure, and $g-C_3N_4$, with a graphitic-based layered structure, can interact at the crystal level when combined [15]. The crystalline compatibility between these two materials is crucial to ensure efficient charge transfer and optimal interfacial interaction. Good charge transfer between $BiVO_4$, the main photocatalyst, and $g-C_3N_4$, an auxiliary semiconductor, can enhance the separation of electron-hole charge pairs, improving the photocatalytic activity [16]. The crystalline size of the synthesized sample can be determined based on XRD data.

The results obtained from Table 1 show that the addition of $g-C_3N_4$ to $BiVO_4$ material reduces the crystal size. In other words, $BiVO_4$ crystals become smaller when $g-C_3N_4$ is added. This indicates that $g-C_3N_4$ can influence or control the size of $BiVO_4$ crystals.

This process usually occurs due to the interaction between $g-C_3N_4$ and $BiVO_4$, which influences the crystal growth of $BiVO_4$. The addition of $g-C_3N_4$ may interfere with crystal formation, resulting in smaller crystal sizes. Therefore, it can be concluded that $g-C_3N_4$ acts as an agent that controls or modifies the crystal size of $BiVO_4$ [17].

3.2. Analysis of the Band Gap Energy of $BiVO_4/g-C_3N_4$ Material

Semiconductor materials were characterized using UV-Vis DRS to determine the bandgap energies of $BiVO_4$, $g-C_3N_4$, and $BiVO_4/g-C_3N_4$ composite variations of samples A (1:2), B (1:3), and C (1:4).

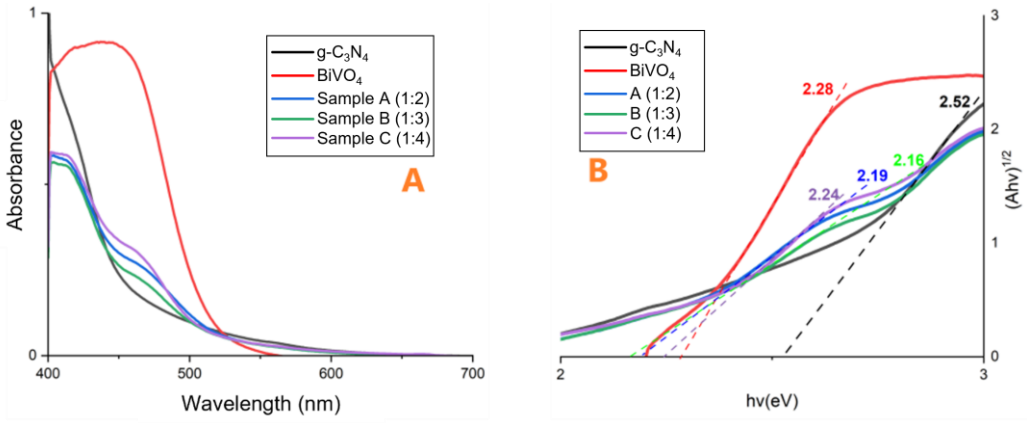

Figure 2. (A) Absorbance spectra and (B) energy levels of $BiVO_4$, g-C_3N_4, and $BiVO_4$/g-C_3N_4

Based on Figure 2, the absorption results indicate that the $BiVO_4$, g-C_3N_4, and $BiVO_4$/g-C_3N_4 composites act as effective adsorbents in the visible wavelength range. The band gap energies were measured as 2.28 eV for $BiVO_4$, 2.52 eV for g-C_3N_4, and 2.19 eV, 2.16 eV, and 2.24 eV for $BiVO_4$/g-C_3N_4 samples A, B, and C, respectively. The band gap energy of the $BiVO_4$/g-C_3N_4 composite decreased compared to that of the pure $BiVO_4$ and g-C_3N_4 samples.

The decrease in band gap energy in $BiVO_4$/g-C_3N_4 composites compared to pure $BiVO_4$ and g-C_3N_4 occurs due to various physical and chemical interactions. In the composite, electron transfer between $BiVO_4$ and g-C_3N_4 and the formation of new energy levels reduce the required excitation energy [18]. Crystal structure distortions and defects that appear when two materials are mixed also contribute to the decrease in band gap energy. In addition, quantum confinement effects on nano-sized particles and interfacial influences between the two materials create additional lower energy levels. Charge redistribution at the interface also affects the distribution of energy levels. All these factors collectively decrease the band gap energy of the $BiVO_4$/g-C_3N_4 composite, increasing its efficiency in absorbing visible light for applications such as photocatalysis or optoelectronics [19].

3.3. Morphology of $BiVO_4$/g-C_3N_4

Morphological analysis of a material is carried out to understand its surface properties, which can be reviewed from particle size, channel, pore, shape, and composition. Based on Figure 3, the morphology formed in sample A forms a rod or rod-like. The B sample has a morphology consisting of large particles that are irregular and fine. From the SEM results shown in Figure 3, it can be concluded that the $BiVO_4$/g-C_3N4 composite has been successfully formed, as indicated by the piled sheets on the surface, which are characteristic of g-C_3N_4. This can be seen from the morphology formed in sample C, which indicates the presence of a combination of sheets and rods or rod-likes. The interaction between the $BiVO_4$ and g- C_3N_4 crystals suggests that both components have been integrated into a new structure.

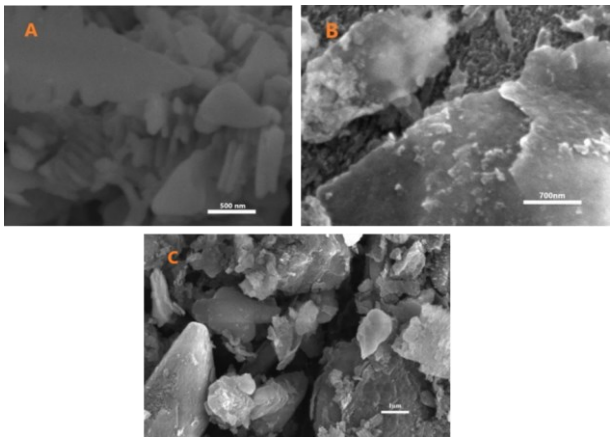

Figure 3. Morphological analysis results of (A) $BiVO_4$ at 25,000× magnification, (B) g-C_3N_4 at 25,000× magnification, (C) $BiVO_4$/g-C_3N_4 at 10,000× magnification

The morphology observed in samples A, B, and C significantly influences the material's photocatalytic efficiency. Sample A, with its rod-like structure, offers a large surface area and short paths for electron and hole movement, which reduces the likelihood of recombination and enhances photocatalytic efficiency. Sample B exhibits a large, irregular, and smooth particle morphology, with sheets of g-C_3N_4 piled up on the surface. While this structure provides numerous active sites for photocatalytic reactions, the large particle size may negatively impact light absorption and reactant diffusion [20].

Sample C shows a combined morphology of g-C_3N_4 sheets and $BiVO_4$ rods, signifying that the two components have been well integrated into the composite structure. This integration results in synergistic interactions that enhance charge separation and reduce recombination, which is critical to photocatalytic efficiency. These combined sheets and rods also provide more active sites and increase light absorption in the broader spectrum. Therefore, the $BiVO_4$/g-C_3N_4 composite in sample C most likely exhibits the best photocatalytic efficiency, utilizing the advantages of both morphologies to improve the photocatalyst performance [21].

3.4. Identification of the Optimum pH for MB Degradation

Determining the optimal pH value in the degradation process aims to understand the influence of dye pH on the adsorption and photocatalytic performance of $BiVO_4$/g- C_3N_4 materials. The analysis results in Figures 4 and 5 indicate that adsorption activity increases with increasing alkalinity. Meanwhile, photocatalytic activity increases from pH 3 to 7 but decreases when pH is above 7 due to increased adsorption activity, which reduces the active surface of the photocatalyst.

MB, a cationic dye with a pKa of approximately 3.8, readily releases protons under acidic conditions. This low pKa value indicates that MB remains in its cationic, or positively charged, form even at higher pH levels [22]. This is due to the very low pKa of MB, which means that typical alkaline pH levels are insufficient to cause significant proton loss. In other words, even in an alkaline environment, MB maintains its positive charge, as its pKa indicates stability in its cationic form across the relevant pH range [23].

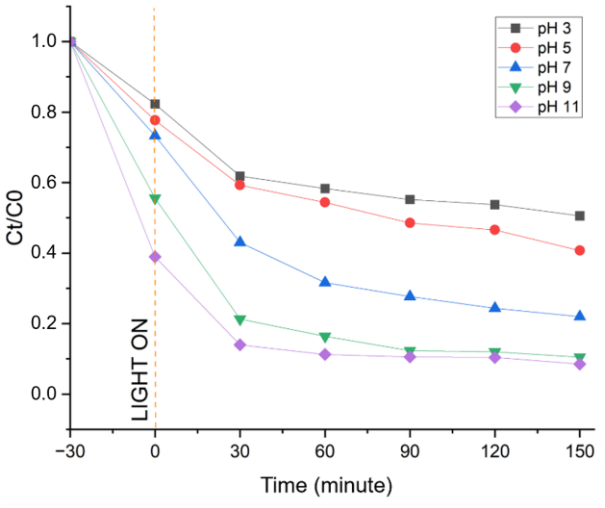

Figure 4. Graph of the effect of pH on the MB adsorption

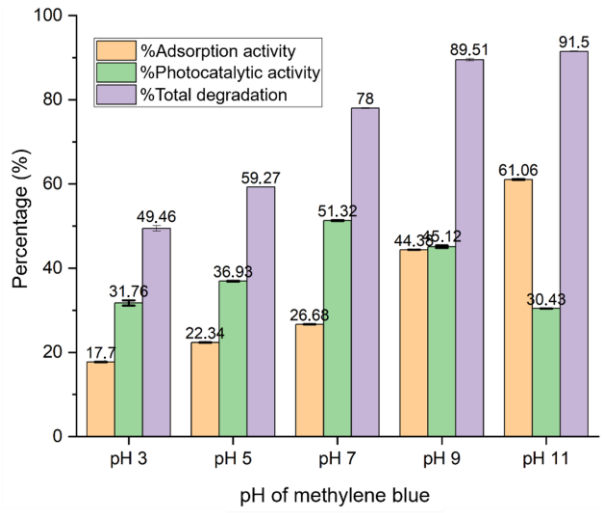

Figure 5. Graph of adsorption activity, photocatalytic activity, and degradation efficiency percentages of $BiVO_4$/g-C_3N_4 in MB degradation

The analysis indicates that the adsorption activity of the $BiVO_4$/g-C_3N_4 photocatalyst is affected by the pH of the environment, as the photocatalyst's charge varies with pH. With a pHpzc of 3.46, the photocatalyst tends to acquire a negative charge at pH levels above 3.46 [24]. Under alkaline conditions (pH > 3.46), the negative charge on the photocatalyst enhances electrostatic attraction towards positively charged dyes such as MB, thereby improving the dye's adsorption onto the photocatalyst. Conversely, at pH levels below 3.46 (acidic conditions), the photocatalyst tends to acquire a positive charge, which competes with the cationic MB.

This results in weaker electrostatic attraction between the photocatalyst and the dye, leading to reduced or even unsuccessful adsorption of MB onto the photocatalyst surface [25]. Additionally, research by Ouyang *et al.* [26] on the effect of pH on the adsorption activity of g-C_3N_4 found that increasing pH leads to an increase in both the pore size and surface area of g-C_3N_4. The increase in specific surface area and pore volume of g-C_3N_4 is beneficial to the adsorption of pollutant molecules and provides more active sites for photocatalytic degradation.

The photocatalytic activity increases from pH 3 to 7 but decreases at pH above 7. This is due to the increased adsorption activity that fills the pores and active surface of the photocatalyst, reducing the amount of surface available for photocatalysis reactions. In addition, high adsorption activity also reduces the photon adsorption efficiency of the photocatalyst, thus decreasing its effectiveness [27].

3.5. Identification of the Optimum Degradation Time

The optimal degradation time was determined to assess the effectiveness of $BiVO_4$/g-C_3N_4 composites. This was done by observing changes in the photocatalytic degradation activity of MB at 30, 60, 90, 120, 150, 180, and 210 minutes. Figure 6 shows that as the irradiation time increases, the percentage of MB degradation also rises. In this study, MB degradation increased from 30 to 150 minutes. Initially, energetic photons hit the photocatalyst, generating free electrons and holes within the semiconductor structure. These free electrons subsequently produce reactive oxygen species (ROS), such as hydroxyl radicals (OH·) and superoxide ions (O_2·$^-$), which are highly reactive [28].

The longer the contact time between the photocatalyst and organic pollutants, the more photons are absorbed, generating additional free electrons and holes and increasing the formation of ROS radicals [29]. This explains the observed increase in MB degradation with prolonged contact time. In contrast, organic pollutants without a photocatalyst undergo photolysis, where they absorb photons more slowly and less efficiently, leading to less effective degradation [30]. Thus, photocatalysis proves to be more effective for degrading organic pollutants. ROS radicals are crucial in accelerating the oxidative reactions of organic pollutants, transforming them into simpler and less harmful compounds.

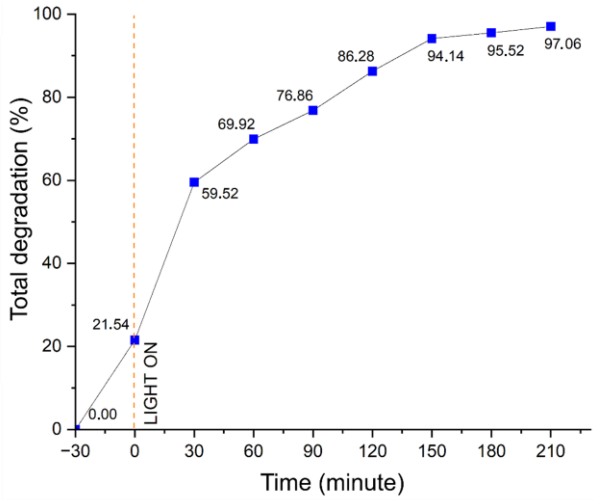

Figure 6. Graph of %total degradation MB by $BiVO_4$/g- C_3N_4

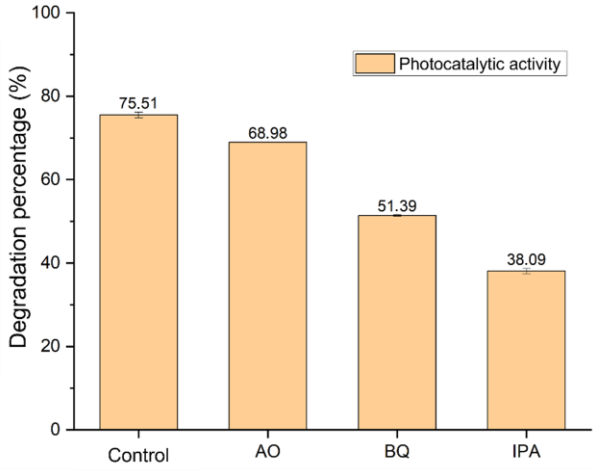

Figure 7. Graph of the material degradation mechanism of $BiVO_4$/g-C_3N_4

After 180 minutes, the degradation rate plateaued and tended to stabilize. This stabilization occurs because the remaining MB is minimal while intermediate compounds (intermediates) increase. ROS radicals are also involved in degrading these MB intermediates [31]. Consequently, 150 minutes was selected as the optimal degradation time, achieving a degradation percentage of 94.14%. Other factors influencing the process include the potential recombination of electrons and holes on the material surface, which converts energy into heat, and the adsorption of MB by the material, which affects the intensity of light reaching the surface [32]. Further research is needed to explore the effects of photocatalyst mass, MB concentration, and light intensity.

3.6. Identification of Active Species in $BiVO_4$/g-C_3N_4 Photocatalysts

Identifying active species helps determine which radical species (·OH, h+, $\cdot O_2^-$) play a more dominant role in degrading MB. This identification is achieved by adding scavengers or sacrificial agents [33]. According to the analysis results shown in Figure 7, photocatalytic activity in MB degradation varies depending on the type of scavenger used. The addition of isopropyl alcohol (IPA) resulted in a degradation value of 38.09%, while benzoquinone (BQ) led to a degradation value of 51.39%. The highest degradation value of 68.98% was achieved by adding ammonium oxalate (AO).

Figure 7 shows that the largest decrease in degradation value occurred with the addition of IPA, which indicates that hydroxyl radicals (·OH) are the main radical species that contribute to the photocatalytic process of MB degradation. These ·OH radicals can be generated through the oxidation of H_2O molecules and adsorbed OH- ions by holes in the valence band [7]. This is evidenced by the smallest degradation value observed with the addition of AO, indicating that the role of holes in the photocatalytic degradation of MB is less dominant compared to other radical species. In addition to the ·OH radical, another radical species that is also influential in the photodegradation of MB is the superoxide radical ($\cdot O_2^-$). The data indicate that the addition of BQ scavengers leads to a decrease in photocatalytic activity. This is because the BQ scavenger captures $\cdot O_2^-$ radicals generated by the photocatalyst, thereby reducing the number of $\cdot O_2^-$ radicals available for MB degradation.

Thus, it can be concluded that the photocatalytic activity by $BiVO_4$/g-C_3N_4 is dominated by the presence of ·OH radicals, as supported by the research of Xiao *et al.* [34]. The ·OH radical plays a significant role in the degradation process, while the $\cdot O_2$- radical also has a contribution although not as great as the ·OH radical.

4. Conclusion

This study successfully synthesized the $BiVO_4$/g- C_3N_4 composite and evaluated its degradation ability towards methylene blue. XRD characterization showed that $BiVO_4$ exhibits a monoclinic phase, g-C_3N_4 has a hexagonal phase, and the $BiVO_4$/g-C_3N_4 composite combines both phases. UV-Vis DRS indicated that the composite has a smaller band gap than the individual components, suggesting enhanced light absorption and photocatalytic efficiency. The optimal conditions for degradation were pH 7 and 150 minutes, with hydroxyl (·OH) radicals being the dominant active species. The incorporation of g-C_3N_4 into $BiVO_4$ formed a heterojunction that significantly improved photocatalytic efficiency. Further research could focus on optimizing the composition ratio, assessing stability and recyclability, and exploring applications for other contaminants and integration into renewable energy systems, potentially advancing waste processing and environmental purification.

Acknowledgment

We thank Jenderal Soedirman University through the Research Grant of "*Riset Dasar* Unsoed," contract number 27.157/UN23.37/PT.01.03/II/2023.

References

[1] Idrees Khan, Khalid Saeed, Ivar Zekker, Baoliang Zhang, Abdulmajeed H. Hendi, Ashfaq Ahmad, Shujaat Ahmad, Noor Zada, Hanif Ahmad, Luqman Ali Shah, Tariq Shah, Ibrahim Khan, Review on Methylene Blue: Its Properties, Uses, Toxicity and Photodegradation, *Water*, 14, 2, (2022), 242 https://doi.org/10.3390/w14020242

[2] Ali H. Jawad, Ahmed Saud Abdulhameed, Mohd Sufri Mastuli, Acid-factionalized biomass material for methylene blue dye removal: a comprehensive adsorption and mechanism study, *Journal of Taibah University for Science*, 14, 1, (2020), 305-313 https://doi.org/10.1080/16583655.2020.1736767

[3] Kingsley O. Iwuozor, Joshua O. Ighalo, Lawal Adewale Ogunfowora, Adewale George Adeniyi, Chinenye Adaobi Igwegbe, An empirical literature analysis of adsorbent performance for methylene blue uptake from aqueous media, *Journal of Environmental Chemical Engineering*, 9, 4, (2021), 105658 https://doi.org/10.1016/j.jece.2021.105658

[4] Salni Salni, Muhammad Said, Eliza Eliza, Anggun Dita Dyah Gayatri, Poedji Loekitowati Hariani, Preparation of $CoFe_2O_4/SiO_2$/Ag Magnetic Composite as Photocatalyst for Congo Red Dye and Antibacterial Potential, *Jurnal Kimia Sains dan Aplikasi*, 25, 7, (2022), 235-244 https://doi.org/10.14710/jksa.25.7.235-244

[5] Dessy Ariyanti, Afiatin Afiatin, Pury Diana Shintawati, Aprilina Purbasari, TiO_2-PDMS Super Hydrophilic Coating with Self-Cleaning and Antimicrobial Properties, *Jurnal Kimia Sains dan Aplikasi*, 24, 6, (2021), 192-199 https://doi.org/10.14710/jksa.24.6.192-199

[6] M. Ganeshbabu, N. Kannan, P. Sundara Venkatesh, G. Paulraj, K. Jeganathan, D. MubarakAli, Synthesis and characterization of $BiVO_4$ nanoparticles for environmental applications, *RSC Advances*, 10, 31, (2020), 18315-18322 https://doi.org/10.1039/D0RA01065K

[7] Bingjun Jin, Yoonjun Cho, Cheolwoo Park, Jeehun Jeong, Sungsoon Kim, Jie Jin, Wooyul Kim, Luyang Wang, Siyu Lu, Shengli Zhang, Sang Ho Oh, Kan Zhang, Jong Hyeok Park, A two-photon tandem black phosphorus quantum dot-sensitized $BiVO_4$ photoanode for solar water splitting, *Energy & Environmental Science*, 15, 2, (2022), 672-679 https://doi.org/10.1039/D1EE03014K

[8] Diksha Mittal, Dimple P. Dutta, Synthesis, structure, and selected photocatalytic applications of graphitic carbon nitride: a review, *Journal of Materials Science: Materials in Electronics*, 32, 14, (2021), 18512-18543 https://doi.org/10.1007/s10854-021-06508-y

[9] Sry Wahyuni, Syukri Syukri, Syukri Arief, Green synthesis of Ag/TiO_2 Nanocomposite Assisted by Gambier Leaf (*Uncaria gambir* Roxb) Extract, *Jurnal Kimia Sains dan Aplikasi*, 22, 6, (2019), 250-255 10.14710/jksa.22.6.250-255

[10] Muhammad Salim Mansha, Tahir Iqbal, Muhammad Farooq, Khalid Nadeem Riaz, Sumera Afsheen, Muhammad Shehzad Sultan, Nabil Al-Zaqri, Ismail Warad, Arslan Masood, Facile hydrothermal synthesis of $BiVO_4$ nanomaterials for degradation of industrial waste, *Heliyon*, 9, 5, (2023), https://doi.org/10.1016/j.heliyon.2023.e15978

[11] Debajyoti Das, Pronay Makal, RETRACTED: Narrow band gap reduced TiO_2-B:Cu nanowire heterostructures for efficient visible light absorption, charge separation and photocatalytic degradation, *Applied Surface Science*, 506, (2020), 144880 https://doi.org/10.1016/j.apsusc.2019.144880

[12] Syed Khasim, Apsar Pasha, Mohana Lakshmi, Chellasamy Panneerselvam, Mohammad Fahad Ullah, A. A. A. Darwish, Taymour A. Hamdalla, S. Alfadhli, S. A. Al-Ghamdi, Synthesis of g-C_3N_4/CuO Nanocomposite as a Supercapacitor with Improved Electrochemical Performance for Energy Storage Applications, *International Journal of Electrochemical Science*, 17, 8, (2022), 220838 https://doi.org/10.20964/2022.08.29

[13] Javad Safaei, Habib Ullah, Nurul Aida Mohamed, Mohamad Firdaus Mohamad Noh, Mohd Fairus Soh, Asif A. Tahir, Norasikin Ahmad Ludin, Mohd Adib Ibrahim, Wan Nor Roslam Wan Isahak, Mohd Asri Mat Teridi, Enhanced photoelectrochemical performance of Z-scheme g-C_3N_4/$BiVO_4$ photocatalyst, *Applied Catalysis B: Environmental*, 234, (2018), 296-310 https://doi.org/10.1016/j.apcatb.2018.04.056

[14] Pham Hoai Linh, Pham Do Chung, Nguyen Van Khien, Le Thi Mai Oanh, Vu Thi Thu, Ta Ngoc Bach, Lam Thi Hang, Nguyen Manh Hung, Vu Dinh Lam, A simple approach for controlling the morphology of g-C_3N_4 nanosheets with enhanced photocatalytic properties, *Diamond and Related Materials*, 111, (2021), 108214 https://doi.org/10.1016/j.diamond.2020.108214

[15] Kharisma Madda Ellyana, Kharisma Luthfiaratri Rahayu, Ratri Febriastuti, Abdul Haris, Cassava Skin Usage (*Manihot esculenta* L.) as Photocatalyst for Degradation of Methylene Blue in the River of Textile Industrial Zone, *Jurnal Kimia Sains dan Aplikasi*, 21, 4, (2018), 232-236 https://doi.org/10.14710/jksa.21.4.232-236

[16] Xiaowei Li, Bin Wang, Wenxuan Yin, Jun Di, Jiexiang Xia, Wenshuai Zhu, Huaming Li, Cu^{2+} modified g-C_3N_4 photocatalysts for visible light photocatalytic properties, *Acta Physico-Chimica Sinica*, 36, 1902001, (2020), 10.3866

[17] Binbin Zhao, Wei Zhong, Feng Chen, Ping Wang, Chuanbiao Bie, Huogen Yu, High-crystalline g-C_3N_4 photocatalysts: Synthesis, structure modulation, and H_2-evolution application, *Chinese Journal of Catalysis*, 52, (2023), 127-143 https://doi.org/10.1016/S1872-2067(23)64491-2

[18] Mengfei Lu, Qiaoqiao Li, Chengliang Zhang, Xiaoxing Fan, Lei Li, Yuming Dong, Guoqing Chen, Haifeng Shi, Remarkable photocatalytic activity enhancement of CO_2 conversion over 2D/2D g-C_3N_4/$BiVO_4$ Z-scheme heterojunction promoted by efficient interfacial charge transfer, *Carbon*, 160, (2020), 342-352 https://doi.org/10.1016/j.carbon.2020.01.038

[19] Mojgan Goudarzi, Zaid Hamzah Abdulhusain, Masoud Salavati-Niasari, Low-cost and eco-friendly synthesis of Mn-doped Tl_2WO_4 nanostructures for efficient visible light photocatalytic degradation of antibiotics in water, *Solar Energy*, 262, (2023), 111912 https://doi.org/10.1016/j.solener.2023.111912

[20] Jia Jia, Qiqi Zhang, Keke Li, Yating Zhang, Enzhou Liu, Xin Li, Recent advances on g–C_3N_4–based Z-scheme photocatalysts: Structural design and photocatalytic applications, *International Journal of Hydrogen Energy*, 48, 1, (2023), 196-231 https://doi.org/10.1016/j.ijhydene.2022.09.272

[21] Yile Wang, Dan Yu, Wei Wang, Pin Gao, Shan Zhong, Lishan Zhang, Qiangqiang Zhao, Baojiang Liu, Synthesizing Co_3O_4-$BiVO_4$/g-C_3N_4 heterojunction composites for superior photocatalytic redox activity, *Separation and Purification Technology*, 239, (2020), 116562 https://doi.org/10.1016/j.seppur.2020.116562

[22] Thamrin Azis, La Ode Ahmad, Keke Awaliyah, Laode Abdul Kadir, Study of Kinetics and Adsorption Isotherm of Methylene Blue Dye using Tannin Gel from *Ceriops tagal*, *Jurnal Kimia Sains dan Aplikasi*, 23, 10, (2020), 370-376 https://doi.org/10.14710/jksa.23.10.370-376

[23] Deepshikha Pandey, Achlesh Daverey, Kasturi Dutta, Vinod Kumar Yata, Kusum Arunachalam, Valorization of waste pine needle biomass into biosorbents for the removal of methylene blue dye from water: Kinetics, equilibrium and thermodynamics study, *Environmental Technology & Innovation*, 25, (2022), 102200 https://doi.org/10.1016/j.eti.2021.102200

[24] Pooneh Hemmatpour, Alireza Nezamzadeh-Ejhieh, A Z-scheme CdS/$BiVO_4$ photocatalysis towards Eriochrome black T: An experimental design and mechanism study, *Chemosphere*, 307, (2022), 135925 https://doi.org/10.1016/j.chemosphere.2022.135925

[25] Mahboube Hajiali, Mehrdad Farhadian, Shahram Tangestaninejad, Mohsen khosravi, Synthesis and characterization of Bi_2MoO_6/MIL-101(Fe) as a novel composite with enhanced photocatalytic performance: Effect of water matrix and reaction mechanism, *Advanced Powder Technology*, 33, 5, (2022), 103546 https://doi.org/10.1016/j.apt.2022.103546

[26] Yong Ouyang, Xu Jianquan, Yang Aiyu, Caixia Zhong, Hu Wenjing, Feng Shenglei, Hou Youpeng, Photocatalytic Performance of Alkaline Activated Graphitic Carbon Nitride Under Blue LED Light, *Materials Science*, 28, 2, (2022), 129-137

[27] Usman Qumar, Jahan Zeb Hassan, Rukhsar Ahmad Bhatti, Ali Raza, Ghazanfar Nazir, Walid Nabgan, Muhammad Ikram, Photocatalysis vs adsorption by metal oxide nanoparticles, *Journal of Materials Science & Technology*, 131, (2022), 122-166 https://doi.org/10.1016/j.jmst.2022.05.020

[28] Chencheng Dong, Wenzhang Fang, Qiuying Yi, Jinlong Zhang, A comprehensive review on reactive oxygen species (ROS) in advanced oxidation processes (AOPs), *Chemosphere*, 308, (2022), 136205 https://doi.org/10.1016/j.chemosphere.2022.136205

[29] Hossein Ashrafi, Morteza Akhond, Ghodratollah Absalan, Adsorption and photocatalytic degradation of aqueous methylene blue using nanoporous carbon nitride, *Journal of Photochemistry and Photobiology A: Chemistry*, 396, (2020), 112533 https://doi.org/10.1016/j.jphotochem.2020.112533

[30] Yian Chen, Zhouyang Xiang, Desheng Wang, Jian Kang, Haisong Qi, Effective photocatalytic degradation and physical adsorption of methylene blue using cellulose/GO/TiO_2 hydrogels, *RSC Advances*, 10, 40, (2020), 23936-23943 https://doi.org/10.1039/D0RA04509H

[31] Ameer Baig Ali Baig, Vadamalar Rathinam, Jayanthi Palaninathan, Photodegradation activity of yttrium-doped SnO_2 nanoparticles against methylene blue dye and antibacterial effects, *Applied Water Science*, 10, 2, (2020), 76 https://doi.org/10.1007/s13201-020-1143-1

[32] Suhila Alkaykh, Aïcha Mbarek, Elbashir E. Ali-Shattle, Photocatalytic degradation of methylene blue dye in aqueous solution by $MnTiO_3$ nanoparticles under sunlight irradiation, *Heliyon*, 6, 4, (2020), e03663 https://doi.org/10.1016/j.heliyon.2020.e03663

[33] Fengqiu Yu, Fuzhong Gong, Qifan Yang, Yanfeng Wang, Fabrication of a magnetic retrievable dual Z-scheme g-C_3N_4/$BiVO_4$/$CoFe_2O_4$ composite photocatalyst with significantly enhanced activity for the degradation of rhodamine B and hydrogen evolution under visible light, *Diamond and Related Materials*, 125, (2022), 109004 https://doi.org/10.1016/j.diamond.2022.109004

[34] Jiadong Xiao, Yongbing Xie, Jabor Rabeah, Angelika Brückner, Hongbin Cao, Visible-Light Photocatalytic Ozonation Using Graphitic C_3N_4 Catalysts: A Hydroxyl Radical Manufacturer for Wastewater Treatment, *Accounts of Chemical Research*, 53, 5, (2020), 1024-1033 https://doi.org/10.1021/acs.accounts.9b00624